Supporting Information

Improved Efficacy and Reduced Toxicity Using a Custom-Designed Irinotecan-Delivering Silicasome for Orthotopic Colon Cancer

Xiangsheng Liu[1,2,⊥], Jinhong Jiang[2,⊥], Ryan Chan[1], Ying Ji[1], Jianqin Lu[1,2], Yu-Pei Liao[1], Michael Okene[1], Joshua Lin[1], Paulina Lin[1], Chong Hyun Chang[2], Xiang Wang[2], Ivanna Tang[1], Emily Zheng[1], Waveley Qiu[1], Zev A. Wainberg[3], Andre E. Nel[1,2,4]*and Huan Meng[1,2,4]*

[1]Division of NanoMedicine, Department of Medicine, University of California, Los Angeles, 90095 CA, USA.

[2]Center for Environmental Implications of Nanotechnology, California NanoSystems Institute, University of California, Los Angeles, 90095 CA, USA.

[3]Department of Medicine, University of California, Los Angeles, CA 90095

[4]California NanoSystems Institute, University of California, Los Angeles, CA 90095

*To whom correspondence should be addressed:

hmeng@mednet.ucla.edu

anel@mednet.ucla.edu.

[⊥]X. S. Liu and J. H. Jiang contributed equally to this work.

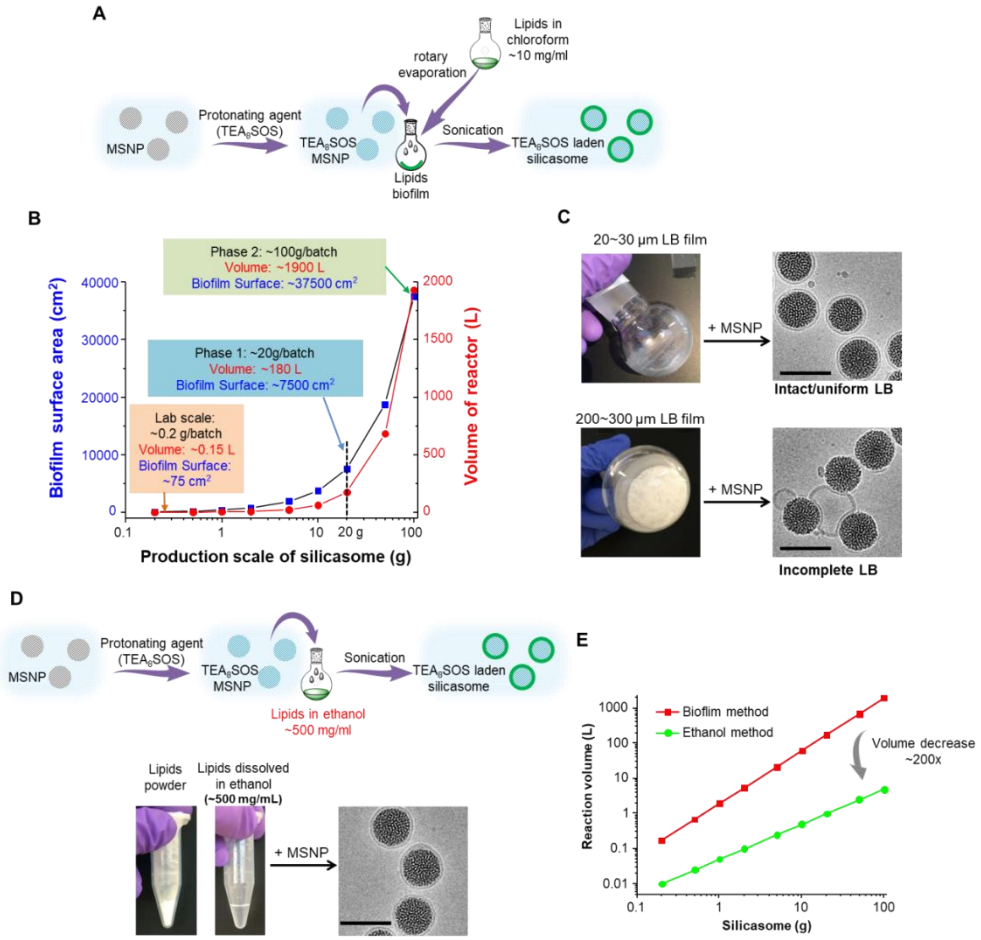

Fig. S1. Customized development of the Ir-silicasome, allowing larger batch production by using an ethanol-exchange method for the lipid bilayer (LB) coating. (A and B) Our previous approach of rapid sealing of MSNP pores through sonication of a biofilm becomes a limiting factor when synthesizing larger particle batches.[1] The biofilm protocol, which utilizes lipid suspension in chloroform at ~10 mg/mL, forms a ~3 mg/cm^2 lipid film with a 20~30 µm thickness.[1] The blue line and red lines in the graphic show the theoretical calculation of the required biofilm surface area and reactor volume for making incremental silicasome batch sizes. For instance, if linearly scaled, this would require, a ~37,500 cm^2 lipid biofilm surface area to coat 100 g MSNP in a 1,900 L flask container. (C) Making use of a more concentrated lipid suspension is also challenging because it results in the formation of a biofilm that is too thick and heterogeneous for the task at hand. This leads to incomplete lipid coating of the MSNP surface, as shown in the cryoEM picture. (D) Bein *et al*. have previously shown, the use of an solvent-exchange method containing ethanol for coating of silica particle surfaces at a low particle working concentration (~1.25 mg/mL).[2] We developed an improved alcohol-exchange method for coating the MSNP surfaces with a simplified process that can work at particle concentrations up to 40 mg/mL. This approach involves the direct introduction of an aqueous suspension of MSNP particles into a concentrated lipid solution in ethanol, followed by controlled energy input through probe sonication. The proposed mechanism of coating is the assembly of the suspended lipid monomers onto on the surfaces of the MSNPs as they are being introduced as an aqueous suspension into the solution (Fig.1D).[3] This approach is advantageous from the perspective that: (i) cryoEM visualization shows complete surface coating of the MSNP by the LB lipid coating (similar to the biofilm approach),[4] (ii) the ethanol exchange method avoids the use of highly toxic chloroform, and (iii) the lipid coating procedure can be used with either conventional probe sonication approach or through the use of a flow cell sonication approach. (E) Collectively, the newly developed alcohol-exchange method dramatically reduced the production volume by ~200 fold compared to the biofilm method. It allowed us to apply lipid coating to incremental batch sizes, ranging from a few hundred mg up to a size of 100 g.

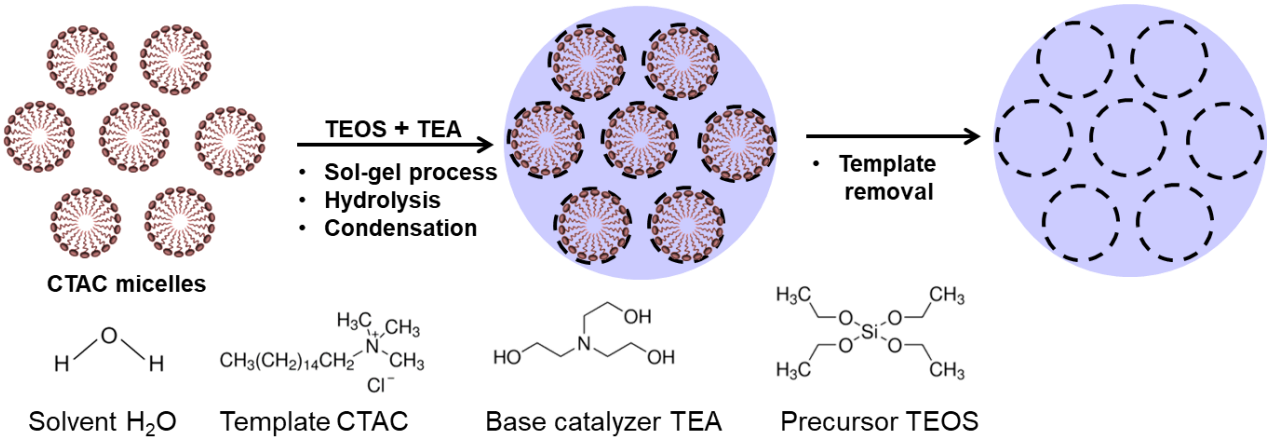

Parameters	Functions
• Precursor TEOS	• Introducing Si source
• Organic base TEA	• Catalyzer to facilitate the reaction
• Templating agent CTAC	• Leads to the formation of porous structure
• Stirring speed	• Determine reaction rate and keep particle uniformity
• Reaction time	• Determine particle size and yield
• Temperature	• Determine rate of reaction

Fig. S2. Upper panel: Schematic to show the steps of MSNP synthesis through a sol-gel synthesis process. Lower panel: Summary of the major parameters required to be controlled for changing the production volume of the sol-gel procedure.

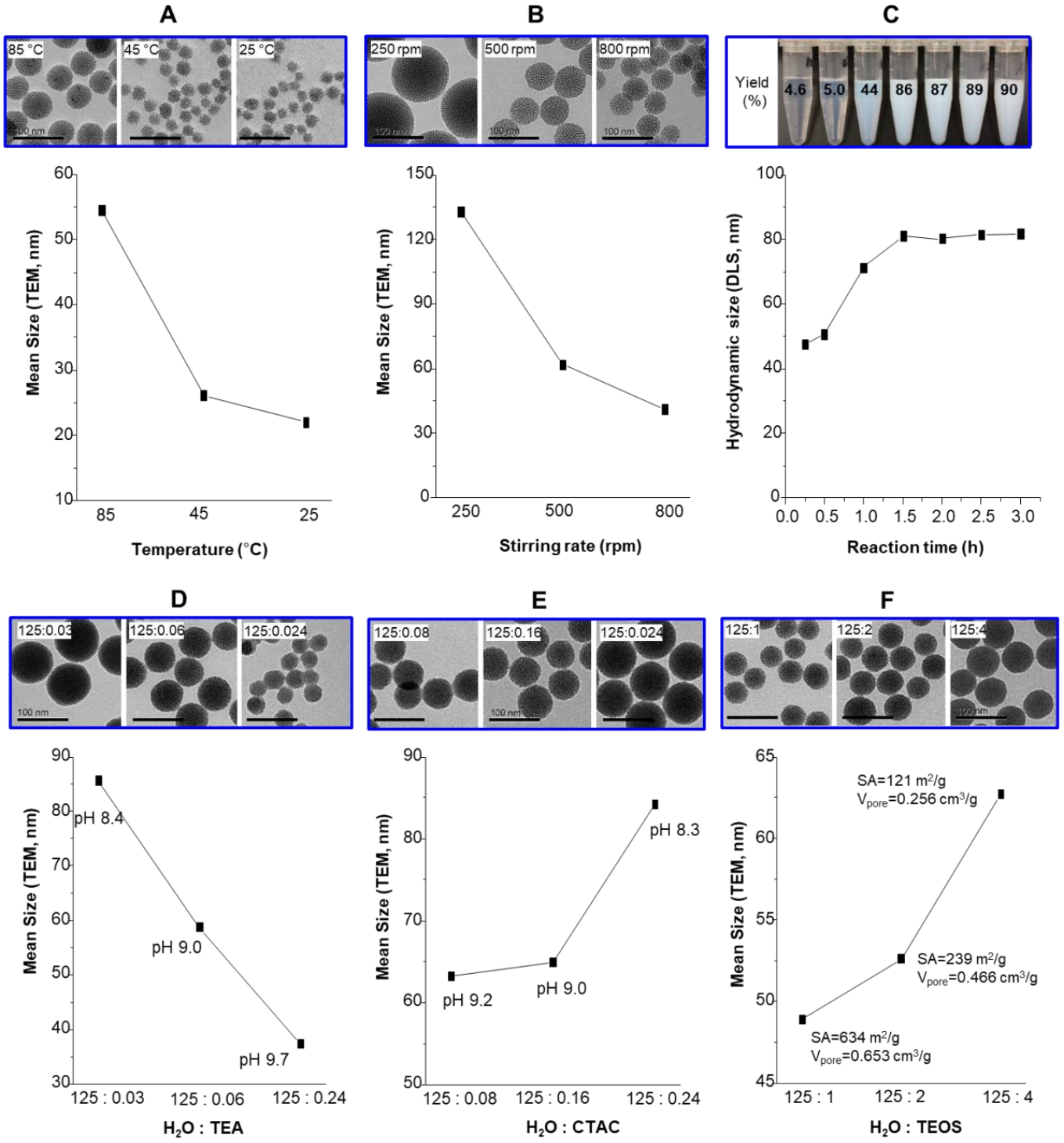

Fig. S3. Examples of adjusting the sol-gel parameters to optimize the large-scale MSNP synthesis by controlling: (A) temperature, (B) stirring speed, (C) reaction time, (D) concentration of the base catalyzer triethanolamine (TEA), (E), concentration of the templating agent, cetyltrimethylammonium chloride (CTAC), and (F) amount of silica precursor tetraethyl orthosilicate (TEOS). (F) in the sol-gel synthesis. The integrated use of these tunable parameters provided a means of optimizing large scale synthesis of MSNPs.

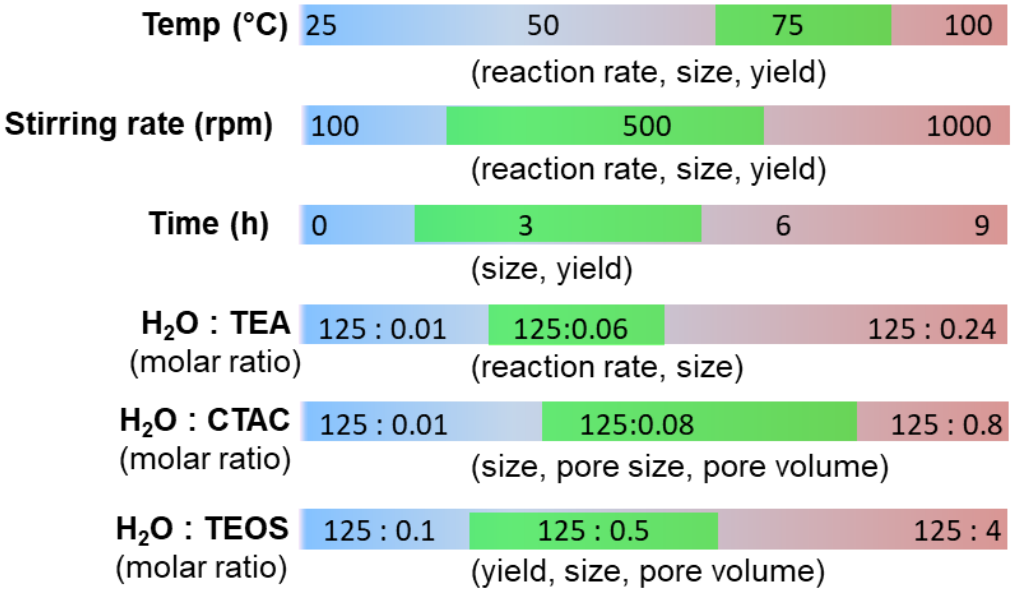

Fig. S4. Utilizing ~70 rounds to optimize MSNP synthesis through a multi-parameter approach, we arrived at a preferred range for each parameter (green) in the synthesis of an ~100 g per batch of bare MSNP in a reaction volume of 18 L. This provides a guideline for the integrated use of multiple MSNP synthesis parameters in tuning the desired MSNP properties, e.g., particle size, morphology, uniformity, pore structure, surface area, pore volume and yield.

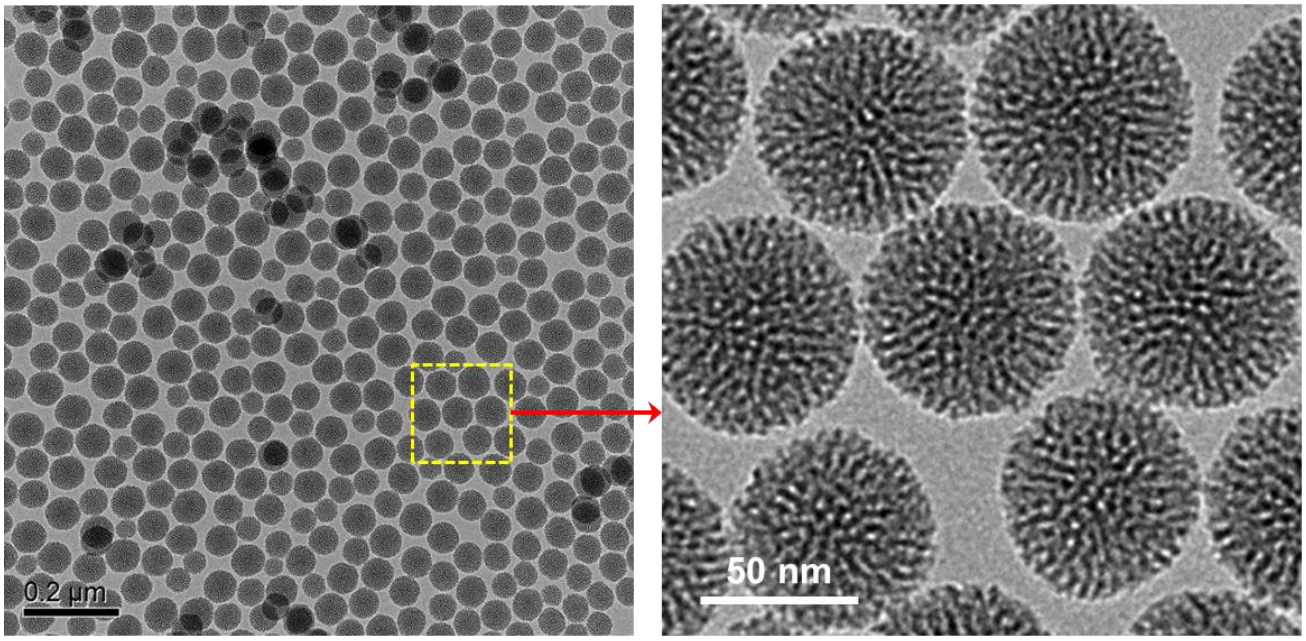

Fig. S5. TEM images of bare MSNP sample synthesized in an ~100 g batch. This batch was prepared in a ~18 L reaction volume as shown in **Fig. 1D.**

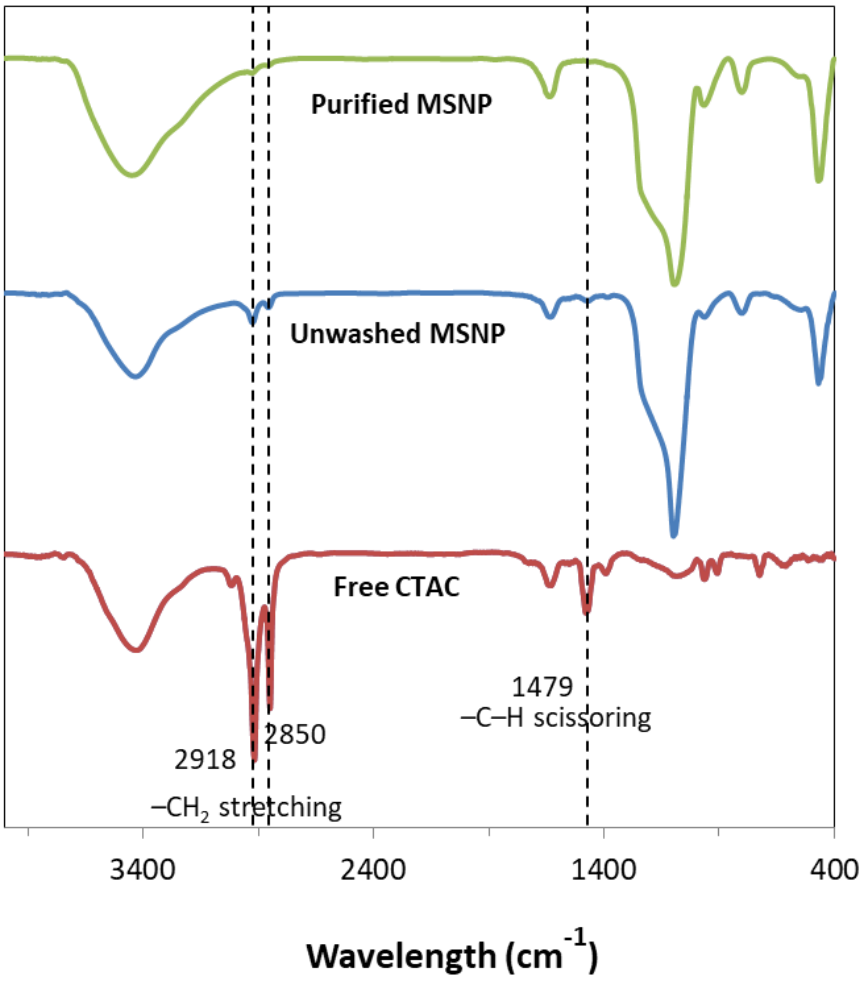

Fig. S6. Besides HPLC quantification, FTIR spectra were used to confirm the effective removal of surfactant (CTAC) before (blue line) and after the use of a series of repetitive washing steps (green line). Free CTAC (red line) was used as a control. The major peaks representing CTAC, *i.e.* the peak for $–CH_2$ stretching (2918 cm^{-1}) and the peak for –C-H scissoring (1479 cm^{-1}), are highlighted by dotted lines.

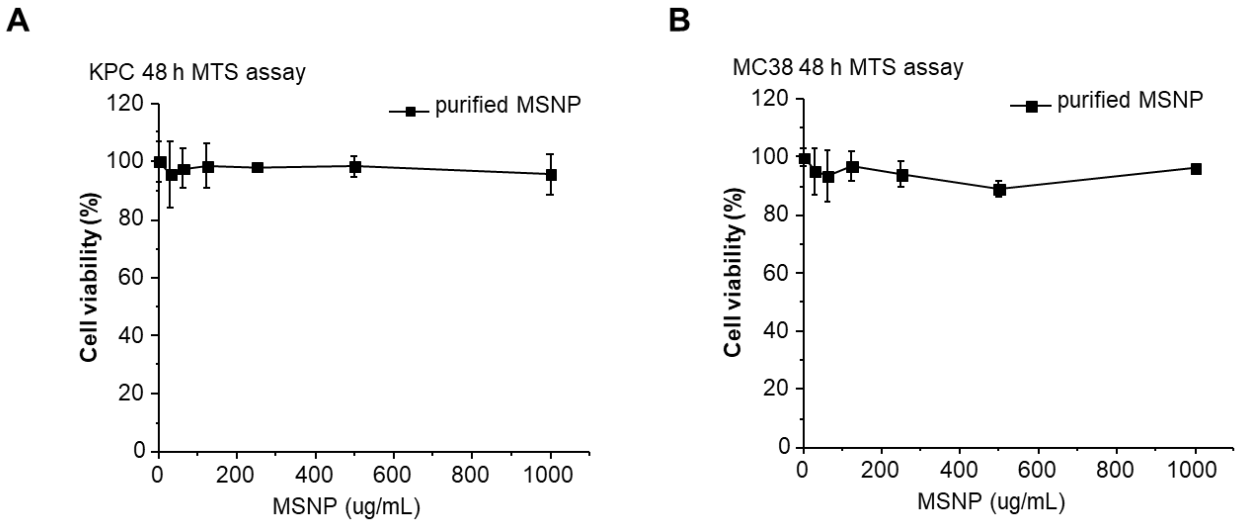

Fig. S7. Cell viability testing, using an MTS assay, to demonstrate the absence of toxicity in KPC and MC38 cell lines, exposed to the purified bare MSNPs at concentrations up to 1,000 μg/mL for 48 h (n = 3, data represent mean ± SD).

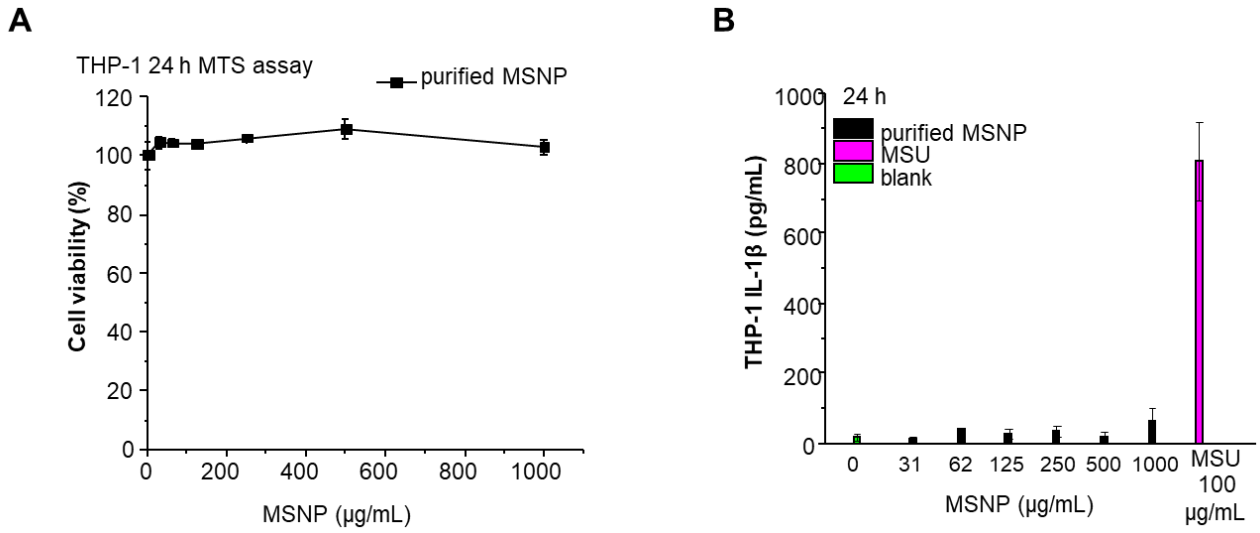

Fig. S8. (A) MTS assay, demonstrating the lack of cytotoxicity of purified bare MSNP, using a concentration up to 1,000 μg/mL over 24 h in THP-1 cells. THP-1 cells are useful for studying IL-1β production, which can be triggered by CTAC (information provided by the NCL at NCI). (B) ELISA assay, demonstrating a lack of release of IL-1β cytokine from THP-1 cells over the same concentration range as in (A). 100 μg/mL monosodium urate (MSU) was used as a positive control. n = 3, data represent mean ± SD. It is also important note that previous testing demonstrated that the coated MSNPs are devoid of biohazard, as determined by elaborate *in vivo* studies for biocompatibility, biodegradability, and bio-elimination of degraded silica.[5–7] We have also previously demonstrated that MSNP synthesis under low temperature conditions do not lead to the formation of highly energetic and strained 3-member siloxane rings that serves as the basis for biopersistant fumed silica toxicity.[8]

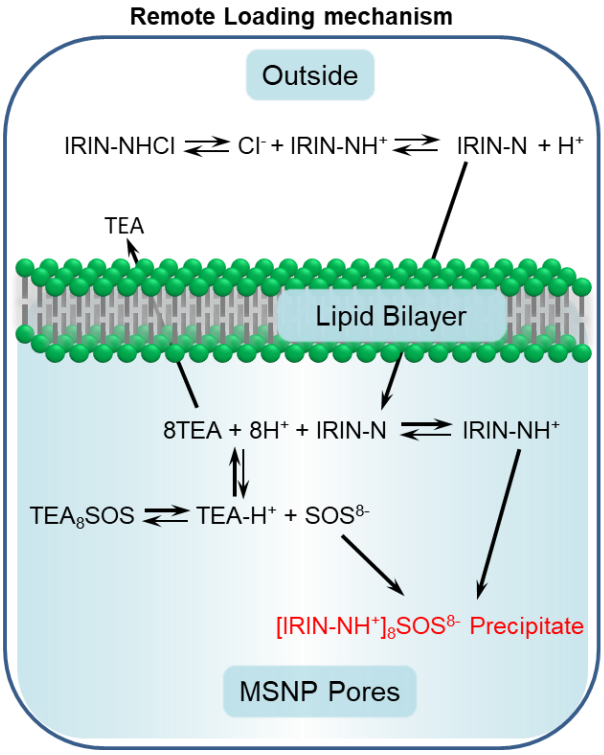

Fig. S9. Schematic to show the mechanism of irinotecan remote loading. The silicasome trapping agent, TEA_8SOS, was incubated in an irinotecan solution, allowing the amphipathic drug to diffuse across the LB. Proton release from the trapping agent converted the encapsulated irinotecan to a hydrophilic derivative that cannot diffuse across the LB. The protonated drug interacts with SOS^{8-} to form a drug precipitate. We have previously identified a comprehensive list of weak basic drugs that can be loaded into silicasome using the proton gradient loading mechanism.[4] The general characteristics of these cargo molecules include properties such as: (i) organic molecular compounds that include primary, secondary, tertiary, or quaternary amine(s); (ii) a pKa <11 to allow protonation and entrapment behind the LB; (iii) water solubility ranging from 5 to 25 mg/mL and amphipathic characteristics that allow diffusion across the LB; (iv) an octanol/water partition coefficient or log P value of -3.0 to 3.0; (v) a molecular weight that is compatible with the geometric size of the MSNP pore size (2-8 nm).

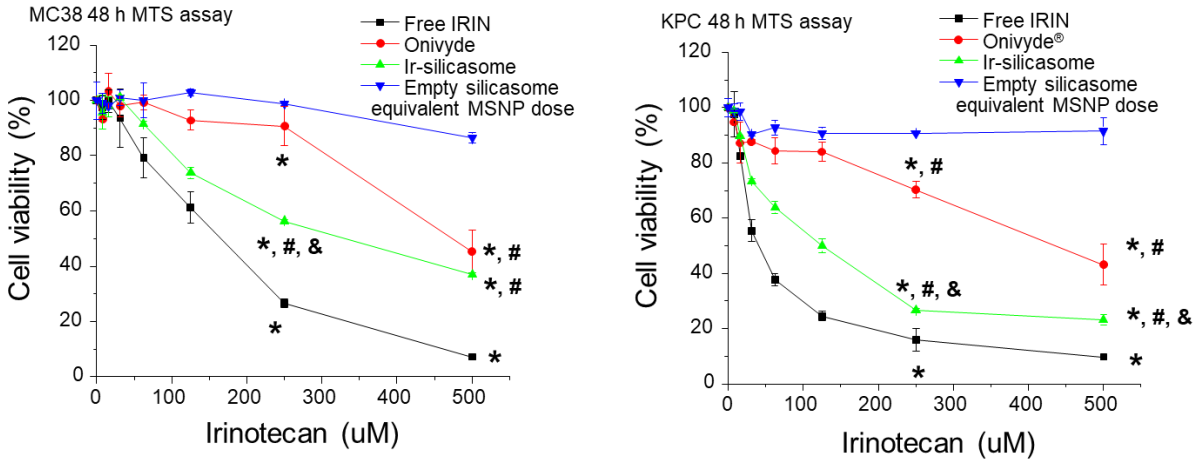

Fig. S10. The *in vitro* killing effects of different irinotecan formulations were evaluated by an MTS assay in both colon cancer MC38 (left) and pancreatic cancer KPC (right) cell lines, exposed to the indicated irinotecan concentrations. The empty silicasome did not show obvious cytotoxicity. n = 3, data represent mean ± SD. *p<0.05 compared to empty silicasome; $^{\#}p$<0.05 compared to free IRIN; $^{\&}p$<0.05 compared to Onivyde® (1-way ANOVA followed by a Tukey's test). The free drug exhibited the most robust killing effect, a finding that is frequently seen in comparative analyses of free *vs* encapsulated chemotherapy agents *in vitro*.[9,10]

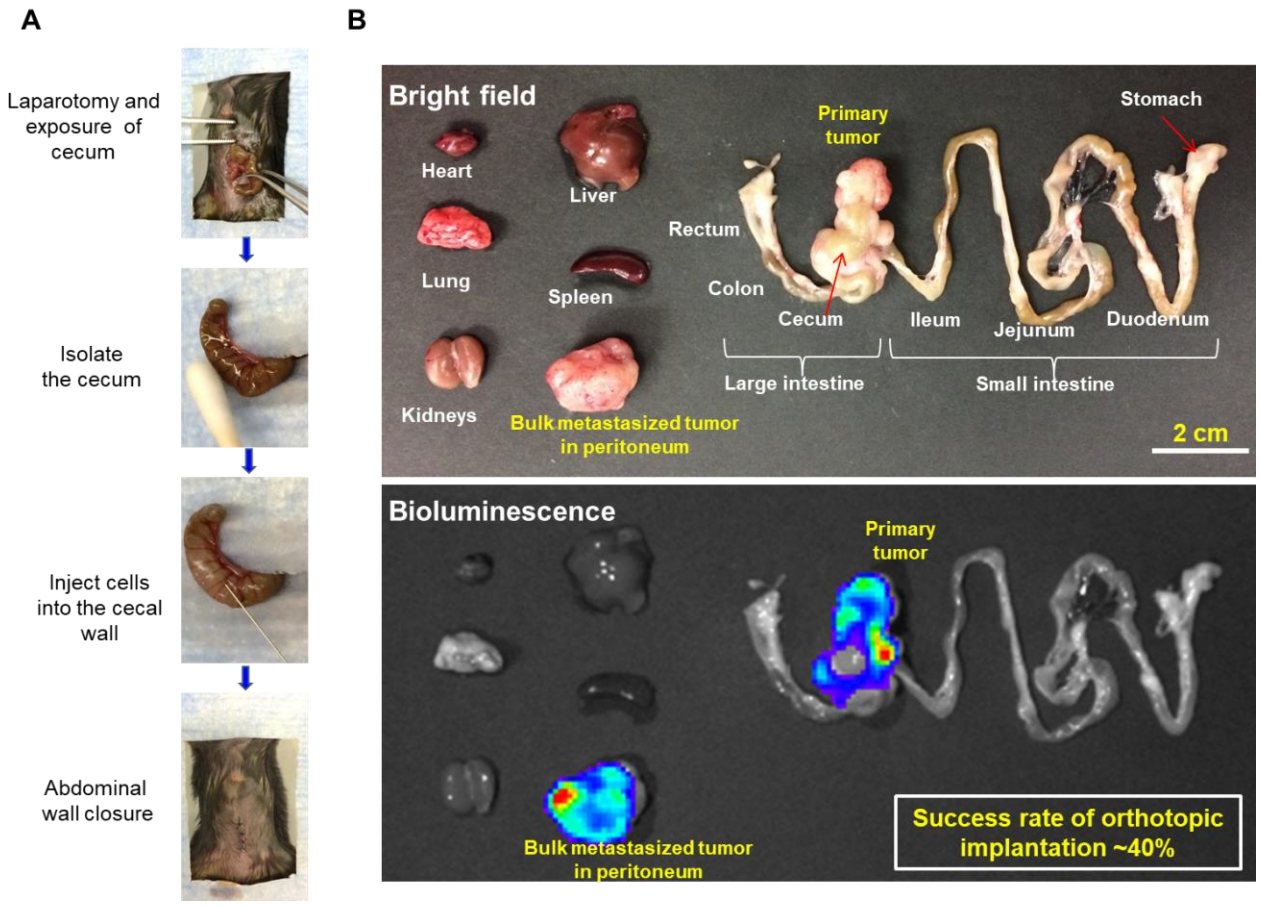

Fig. S11. Characteristics of an orthotopic colon cancer model by injection of MC38-luc cell suspension into the cecum wall. (A) The traditional surgical procedure involves injection of luciferase-expressing MC38 cells between the mucosal and the muscularis layers of the cecum wall in C57BL/6 mice. (B) While this technique is successful for establishing an orthotopic model that resembles the tumor chunk model, as demonstrated in the above autopsy and IVIS imaging results (~4 wks post-surgery), we could only obtain successful tumor engraftment in ~40% mice. This prompted the development of the tumor chunk model which was successful in 95% of animals in our hands (see **Fig. 2**).

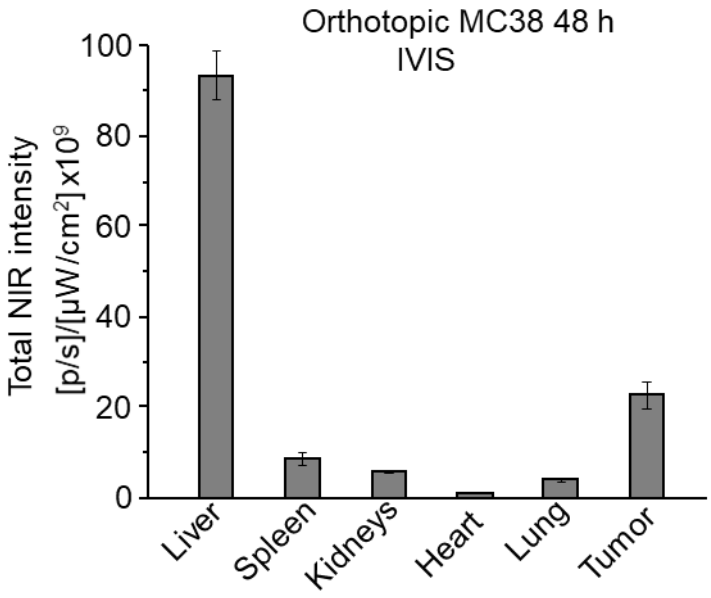

Fig. S12. Quantitative NIR fluorescence intensity analysis for tumors and organs of animals sacrificed at 48 hr after IV injections of DyLight 680 labeled silicasomes in **Fig. 3C**. Animals not injected with particles served as the blank for subtracting background tissue autofluorescence. Data represent mean ± SEM (n=3).

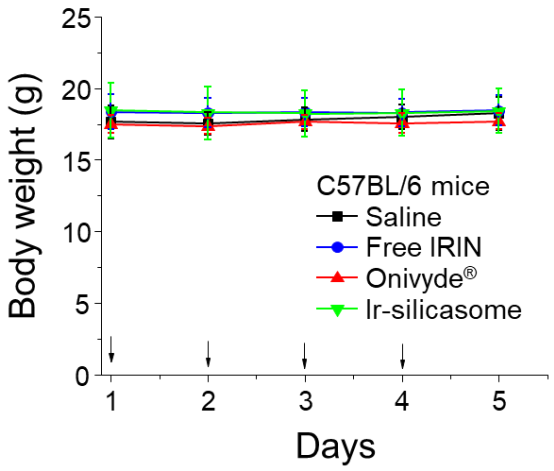

Fig. S13. Body weight profile of animals in the toxicity study described in **Fig. 5.** No obvious body weight change was observed during treatment. Data represent mean ± SD (n=4).

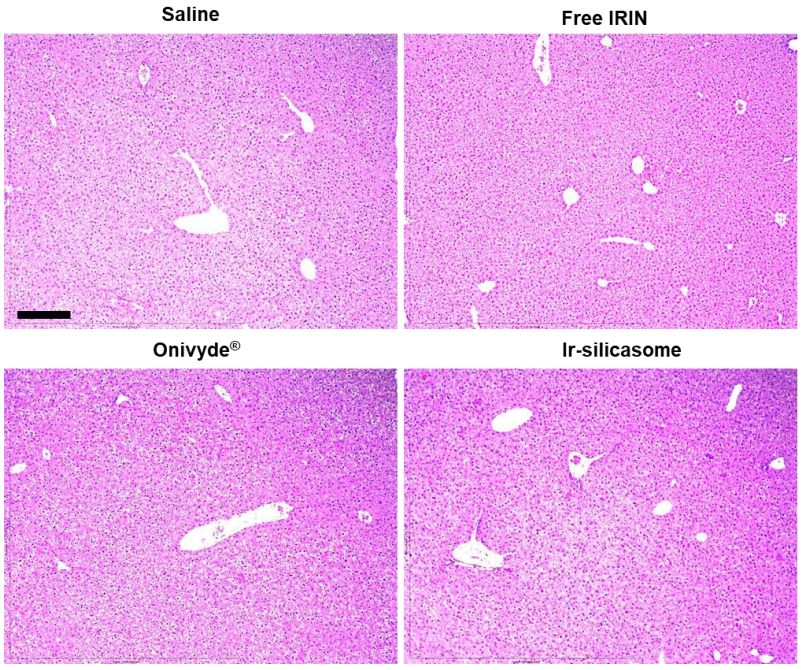

Fig. S14. Representative H&E staining images of liver tissue taken from the animals in the toxicity study in **Fig. 5.** Bar = 200 μm. No obvious liver damage was found in all C57BL/6 mouse strain groups.

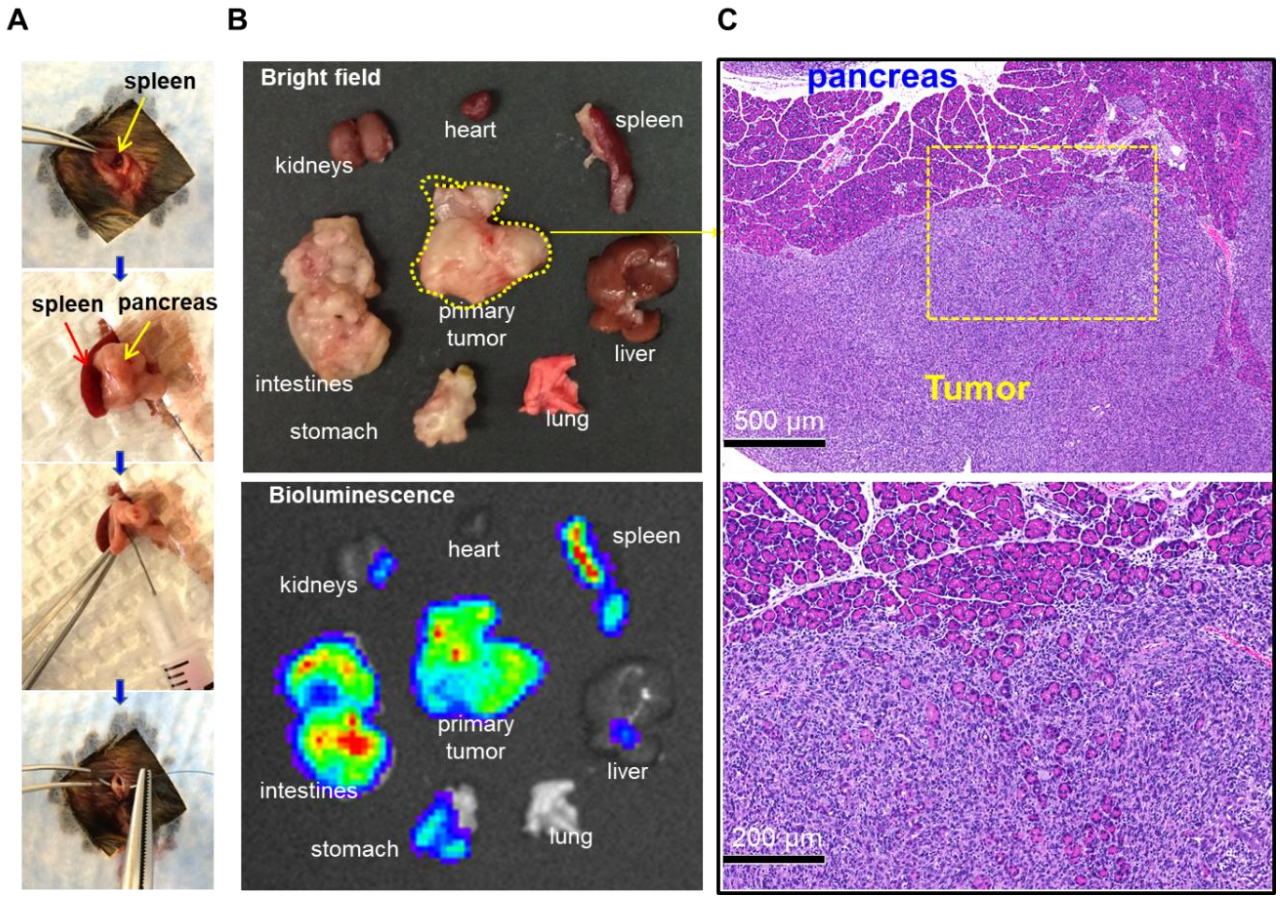

Fig. S15. Illustration of the features of the orthotopic KPC-derived PDAC model in B6/129SF1/J mice. (A) The orthotopic KPC model involves injection of KPC-luc cells into the tail of the pancreas in immunocompetent mice using a rapid surgical procedure, as previously described by us. [4,11] (B) Animal autopsy and IVIS imaging confirm the presence of primary PDAC and its metastasis to a variety of organs. (C) H&E staining of primary tumor tissue confirmed the invasive orthotopic tumor growth.

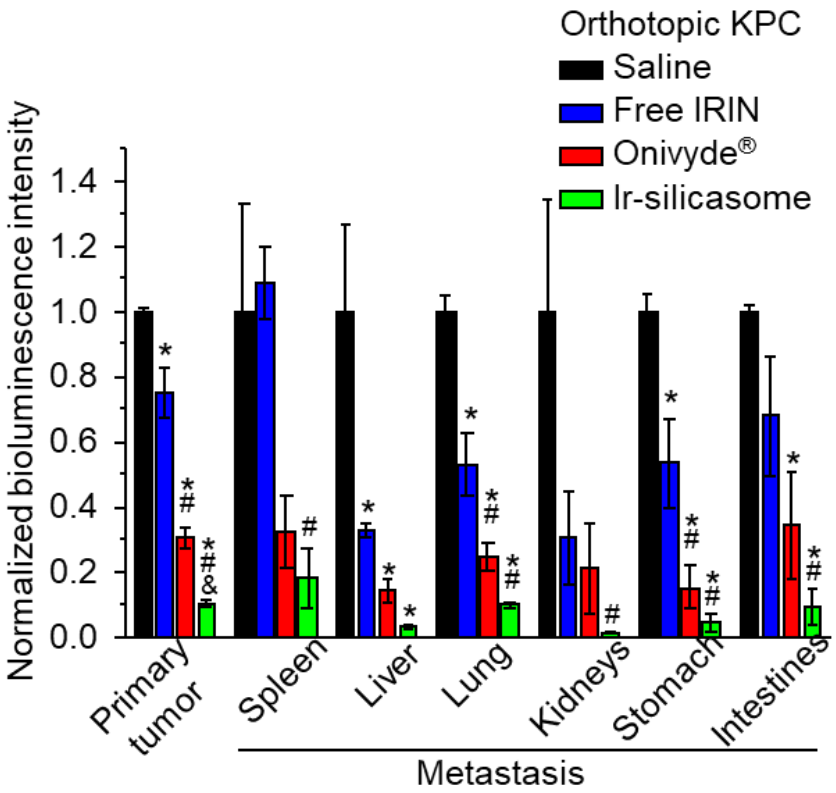

Fig. S16. Quantitative bioluminescence intensity analysis for the primary and metastatic tumors shown in **Fig. 6B**. KPC orthotopic tumor mice (n=3) received three IV injections of free irinotecan, Onivyde® or Ir-silicasome at the same irinotecan dose (40 mg/kg) twice per week. Saline was used as a control. Animals were sacrificed at 24 h after the last treatment. The data represent mean ± SEM, *p<0.05 compared to saline, $^{\#}p$<0.05 compared to free IRIN, $^{\&}p$<0.05 compared to Onivyde® (1-way ANOVA followed by a Tukey's test).

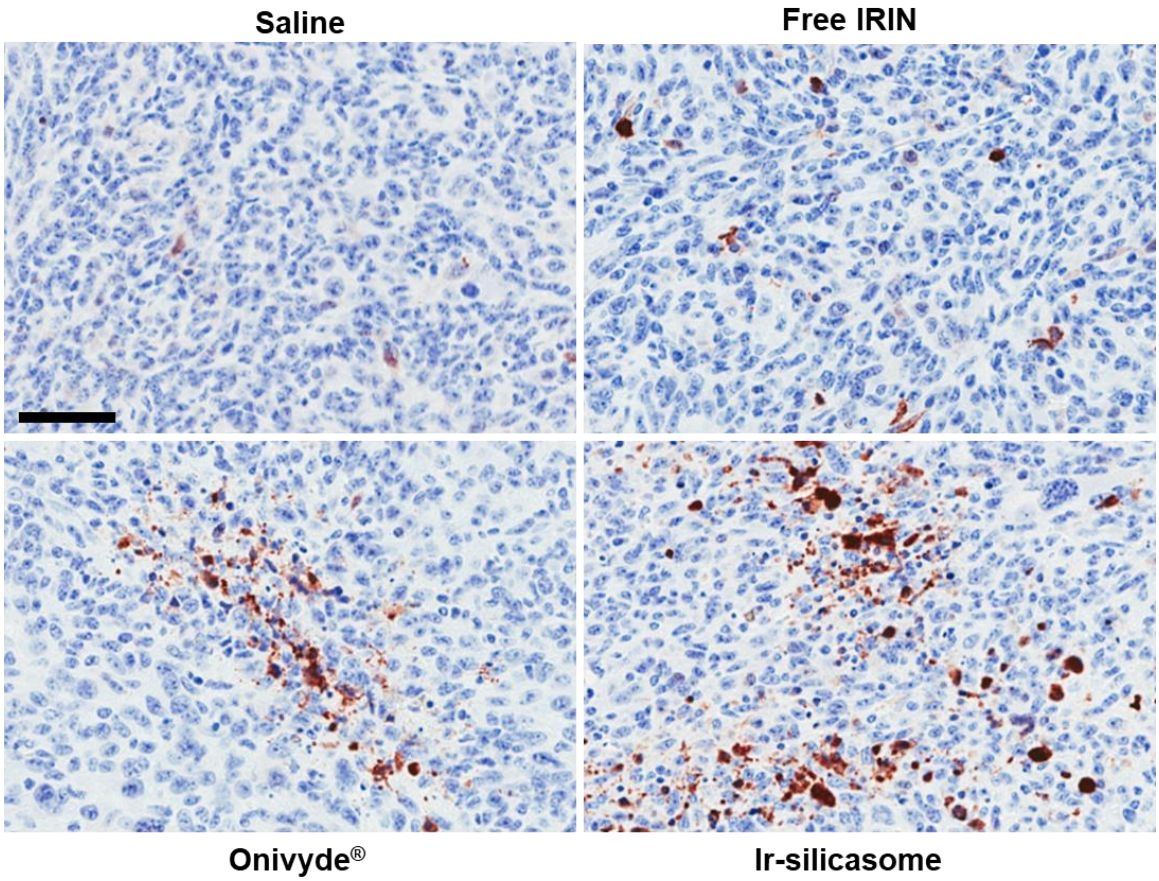

Fig. S17. Representative IHC images of CC-3 (apoptosis marker) staining in primary tumor sections related to the animals in the efficacy study, described in **Fig. 6B.** Bar = 100 μm.

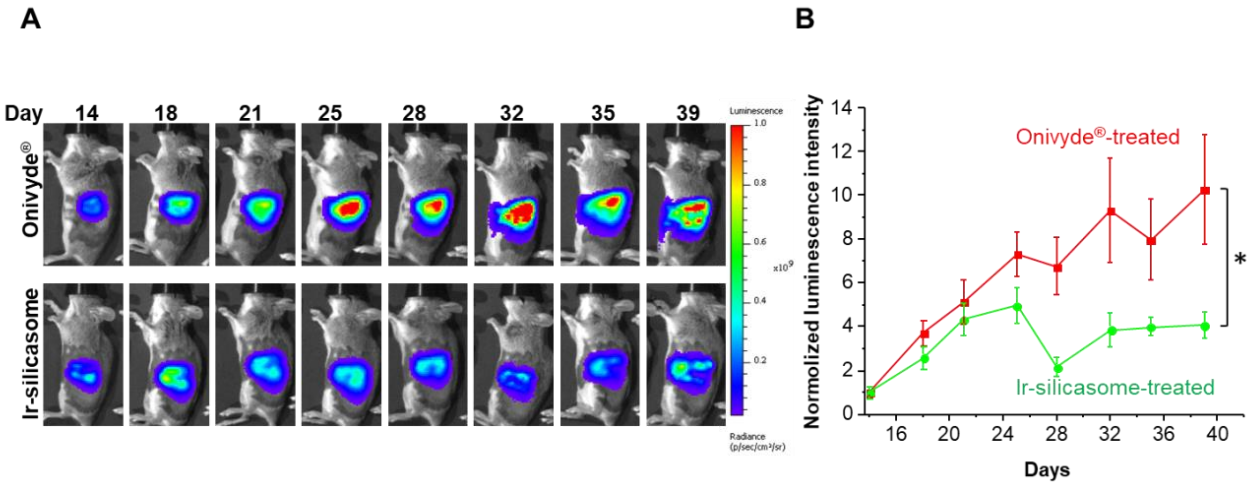

Fig. S18. (A) Representative IVIS imaging of the animals used in the survival study of orthotopic PDAC model in **Fig. 6C.** (B) Tumor bioluminescence intensity was analyzed in the operator defined region-of-interest (ROI). N = 8, data represent mean ± SEM, *p<0.05 (Student's t-test).

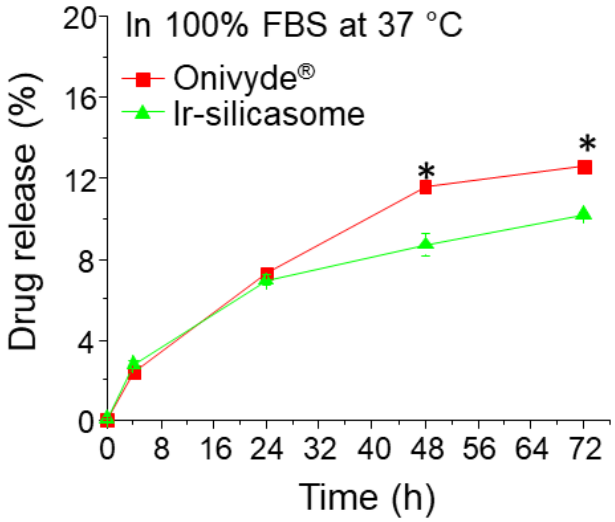

Fig. S19. Irinotecan release profiles from the Onivyde® and Ir-silicasome carriers during incubation in 100% serum at 37 °C for 72 hr, using an irinotecan concentration of 100 µg/mL. Abiotic drug release was analyzed according to our established protocol.[4] The irinotecan concentration was determined by HPLC. Compared to the Ir-silicasome, Onivyde® exhibited a slightly faster rate of release at 48 and 72 hr. N = 3, data represent mean ± SD, *p<0.05 (Student's t-test).

Parameter	Unit	Onivyde	Ir-silicasome
Cmax	μg/ml	602.5±38.6	792.6±114.9
λz	1/h	0.212±0.003	0.072±0.002*
t1/2	h	3.27±0.05	9.60±0.31*
AUC 0-t	μg/ml*h	4299.3±393.4	4848.9±286.4
AUC 0-inf	μg/ml*h	4299.4±393.4	4957±284.0
MRT	h	4.75±0.37	9.63±0.57*
Vz	(ug)/(μg/ml)	0.897±0.103	2.258 ± 0.201*
Cl	(ug)/(μg/ml)/h	0.189±0.019	0.163±0.010

Cmax: maximum plasma concentration; λz: terminal elimination rate; *t*1/2: half-life; AUC: area under the curve; MRT: mean residence time; Vz: volume of distribution; Cl: systemic clearance. * indicate statistical significance ($p < 0.05$).

Table S1. PK parameters for Onivyde and the Ir-silicasome in female C57BL/6 mice after a single IV administration (irinotecan: 40 mg/kg). The PK study was performed as described in **Fig. 3A**. N = 3, data represent mean ± SD, *p<0.05 (Student's *t*-test).

Additional methods:

Cell culture and in vitro cell study: MC38 and KPC cells were cultured in DMEM, containing 10% FBS, 100 U/mL penicillin, 100 μg/mL streptomycin, and 2 mM L-glutamine. THP-1 cells were obtained from ATCC (Manassas, VA) and cultured in RPMI 1640 medium supplemented with 10% FBS.

MTS cytotoxicity assay: The cytotoxicity of purified MSNPs was assessed in a standard MTS assay (CellTiter 96® AQueous One Solution Cell Proliferation Assay, Promega). KPC or MC38 cells were plated at a density of 5×10^3 cells per well in a 96-well plate and cultured for 24 hr. The medium was replaced with fresh medium containing the different NPs at the indicated concentrations. Non-treated cells were used as control. After a 48 hr treatment, the medium was replaced with 100 μL fresh medium containing MTS solution (5:1, v/v medium/ CellTiter 96® Aqueous stock solution) for further culture at 37°C for 1 hr. The absorbance of the culture wells at 490 nm was directly recorded by a microplate reader (M5e, Molecular Device, USA). Wells without cells but contained the same MTS solution were used as blank. The relative cell viability (%) is [(the absorption of treated well - blank)/(the absorption of control well - blank)] ×100.

ELISA to determine IL-1β release from THP-1-cells: ELISA was used to assess IL-1β release, as previously shown by us.[12] Briefly, THP-1 cells in 100 μL of tissue culture medium were plated at a density of 3×10^4 cells per well in a 96-well plate. The cells were treated with 1 μg/mL phorbol 12-myristate 13-acetate (PMA) for 16 h. After replenishment with fresh culture medium, the differentiated THP-1 cells were treated with MSNPs in the presence of 10 ng/mL lipopolysaccharide (LPS) for an additional 24 h. The supernatants were collected for measuring IL-1β by and ELISA kit, according to the manufacturer's instructions (BD Biosciences, San Diego, CA). Concentrations were expressed as pg/mL.

Establishment of orthotopic KPC-derived PDAC tumor model: We have previously described the establishment of a KPC-derived orthotopic tumor model.[4,11] Briefly, female B6/129SF1/J mice were purchased from The Jackson Laboratory, and maintained under pathogen-free conditions. All animal experiments were performed under protocols approved by the UCLA Animal Research Committee. The orthotopic model was developed by injecting 50 μL of DMEM/Matrigel (1:1 v/v) containing 2×10^6 KPC-luc cells into the tail of the pancreas in female B6129SF1/J mice (8~10 weeks) by a rapid surgery procedure.[4,11] The efficacy study was performed in tumor-bearing mice ~2 weeks after implantation, at which point the primary tumors had grown to ~0.5 cm. For the biodistribution experiments, the tumor-bearing mice were used ~2 weeks after tumor implantation, at which point the primary tumors had grown to a size of ~0.8 cm.

Efficacy studies on orthotopic KPC-derived PDAC tumor model: Orthotopic KPC bearing mice were used to determine the anti-tumor efficacy and survival outcome of different irinotecan formulations. In the survival experiment, the animals received IV injections of Onivyde® or Ir-silicasome both at the same irinotecan dose of 40 mg/kg twice every week, for a total of 6 administrations (n=8) (Fig. 6C). We also included additional controls, free drug and saline, in the antitumor efficacy experiment as described in Fig. 6B. Live animal imaging was used to monitor the orthotopic tumor burden twice per week; the tumor burden was quantitatively expressed as bioluminescence intensity in the ROI measured, using software. Drug induced apoptosis was analyzed by CC-3 IHC staining.

References

(1) Meng, H.; Wang, M.; Liu, H.; Liu, X.; Situ, A.; Wu, B.; Ji, Z.; Chang, C. H.; Nel, A. E. Use of a Lipid-Coated Mesoporous Silica Nanoparticle Platform for Synergistic Gemcitabine and Paclitaxel Delivery to Human Pancreatic Cancer in Mice. *ACS Nano* **2015**, *9*, 3540–3557.

(2) Cauda, V.; Engelke, H.; Sauer, A.; Arcizet, D.; Rädler, J.; Bein, T. Colchicine-Loaded Lipid Bilayer-Coated 50 Nm Mesoporous Nanoparticles Efficiently Induce Microtubule Depolymerization upon Cell Uptake. *Nano Lett.* **2010**, *10*, 2484–2492.

(3) Hohner, A. O.; David, M. P. C.; Rädler, J. O. Controlled Solvent-Exchange Deposition of Phospholipid Membranes onto Solid Surfaces. *Biointerphases* **2010**, *5*, 1–8.

(4) Liu, X.; Situ, A.; Kang, Y.; Villabroza, K. R.; Liao, Y.; Chang, C. H.; Donahue, T.; Nel, A. E.; Meng, H. Irinotecan Delivery by Lipid-Coated Mesoporous Silica Nanoparticles Shows Improved Efficacy and Safety over Liposomes for Pancreatic Cancer. *ACS Nano* **2016**, *10*, 2702–2715.

(5) Singh, R. K.; Patel, K. D.; Leong, K. W.; Kim, H.-W. Progress in Nanotheranostics Based on Mesoporous Silica Nanomaterial Platforms. *ACS Appl. Mater. Interfaces* **2017**, *9*, 10309–10337.

(6) Slowing, I.; Viveroescoto, J.; Wu, C.; Lin, V. Mesoporous Silica Nanoparticles as Controlled Release Drug Delivery and Gene Transfection Carriers. *Adv. Drug Deliv. Rev.* **2008**, *60*, 1278–1288.

(7) Tang, F.; Li, L.; Chen, D. Mesoporous Silica Nanoparticles: Synthesis, Biocompatibility and Drug Delivery. *Adv. Mater.* **2012**, *24*, 1504–1534.

(8) Zhang, H.; Dunphy, D. R.; Jiang, X.; Meng, H.; Sun, B.; Tarn, D.; Xue, M.; Wang, X.; Lin, S.; Ji, Z.; Li, R.; Garcia, F.L.; Yang, J.; Kirk, M.L.; Xia, T.; Zink, J.I.; Nel, A.; Brinker, C.J. Processing Pathway Dependence of Amorphous Silica Nanoparticle Toxicity: Colloidal vs Pyrolytic. *J. Am. Chem. Soc.* **2012**, *134*, 15790–15804.

(9) Eliaz, R. E.; Szoka, F. C. Liposome-Encapsulated Doxorubicin Targeted to CD44: A Strategy to Kill CD44-Overexpressing Tumor Cells. *Cancer Res.* **2001**, *61*, 2592–2601.

(10) Alyane, M.; Barratt, G.; Lahouel, M. Remote Loading of Doxorubicin into Liposomes by Transmembrane pH Gradient to Reduce Toxicity toward H9c2 Cells. *Saudi Pharm. J.* **2016**, *24*, 165–175.

(11) Liu, X.; Lin, P.; Perrett, I.; Lin, J.; Liao, Y.-P.; Chang, C. H.; Jiang, J.; Wu, N.; Donahue, T.; Wainberg, Z.; Nel, A.E.; Meng, H. Tumor-Penetrating Peptide Enhances Transcytosis of Silicasome-Based Chemotherapy for Pancreatic Cancer. *J. Clin. Invest.* **2017**, *127*, 2007–2018.

(12) Jiang, W.; Wang, X.; Osborne, O. J.; Du, Y.; Chang, C. H.; Liao, Y.-P.; Sun, B.; Jiang, J.; Ji, Z.; Li, R.; Liu, X.; Lu, J.; Lin, S.; Meng, H.; Xia, T.; Nel, A.E. Pro-Inflammatory and Pro-Fibrogenic Effects of Ionic and Particulate Arsenide and Indium-Containing Semiconductor Materials in the Murine Lung. *ACS Nano* **2017**, *11*, 1869–1883.